

Bonding regimes of nitrogen in amorphous carbon

B. Kleinsorge^{a,*}, A.C. Ferrari^a, J. Robertson^a, W.I. Milne^a, S. Waidmann^b, S. Hearne^c

^a Department of Engineering, University of Cambridge, Cambridge CB2 1PZ, UK

^b Institut für Festkörper- und Werkstofforschung Dresden, Postfach 270016, D-01171 Dresden, Germany

^c National Microelectronics Research Centre, Cork, Ireland

Abstract

Nitrogen can have numerous effects on diamond-like carbon: it can dope, it can form the hypothetical superhard compound C₃N₄, or it can create fullerene-like bonding structures. We studied amorphous carbon nitrogen films deposited by a filtered cathodic vacuum arc as a function of nitrogen content, ion energy and deposition temperature. The incorporation of nitrogen from 10⁻² to 10 at% was measured by secondary ion mass spectrometry and elastic recoil detection analysis and was found to vary slightly sublinearly with N₂ partial pressure during deposition. In the doping regime from 0 to about 0.4% N, the conductivity changes while the sp³ content and optical gap remain constant. From 0.4 to ~10% N, existing sp² sites condense into clusters and reduce the band gap. Nitrogen contents over 10% change the bonding from mainly sp³ to mainly sp². Ion energies between 20 and 250 eV do not greatly modify this behaviour. Deposition at higher temperatures causes a sudden loss of sp³ bonding above about 150°C. Raman spectroscopy and optical gap data show that existing sp² sites begin to cluster below this temperature, and the clustering continues above this temperature. This transition is found to vary only weakly with nitrogen addition, for N contents below 10%. © 2000 Elsevier Science S.A. All rights reserved.

Keywords: Amorphous carbon; Bonding; Carbon nitride; Nitrogen

1. Introduction

This paper describes the structural, optical and electrical properties of nitrogenated amorphous carbon films deposited by a filtered cathodic vacuum arc (FCVA). Films deposited without nitrogen at room temperature generally have very diamond-like properties: a fraction of sp³ bonded carbon atoms up to 85%, high hardness (up to 80 GPa), a resistivity of ~10⁷ (Ω cm)⁻¹ and a band gap of 2–2.5 eV. They are referred to as tetrahedrally bonded amorphous carbon (ta-C) and are distinguished from other diamond-like carbons (DLCs) by the absence of hydrogen.

To investigate the role of nitrogen in a carbon matrix, we have introduced nitrogen as a background gas into the FCVA during deposition. At low N contents, if N enters the ta-C in a sp³ site, it will act as a substitutional dopant [1]. The actual behaviour of nitrogen is complicated because of the presence of both sp³ and sp² C bonding.

To understand the formation of various bonding

types we have also varied the deposition temperature. It is known that ta-C films can only be deposited below a certain temperature, above which graphitic films form [2–4]. At higher nitrogen concentrations and above this temperature fullerene-like carbon films are formed [5,6]. The transition temperature from diamond-like to graphite-like is found to differ in various deposition systems. In this work we aim to investigate the role of nitrogen on the transition temperature.

2. Experimental details

The amorphous carbon films were deposited with a filtered cathodic vacuum arc system described previously [7]. The arc current was kept constant at 75 A and the magnetic field induced by the coils was about 20 mT. This provides a deposition rate of about 7 Å s⁻¹ for pure ta-C. The base pressure of the system was 5 × 10⁻⁷ mbar. Nitrogen was let into the deposition chamber in the region of the filter bend. Samples were simultaneously deposited onto quartz and silicon substrates for optical and conductivity measurements,

* Corresponding author. Fax: +44-01223-332662.

E-mail address: byk20@eng.cam.ac.uk (B. Kleinsorge)

Raman spectroscopy and electron energy loss spectroscopy (EELS). The substrates could be biased with either a DC voltage or, in case of insulating substrates, given a self-bias by applying a high frequency to the substrate holder. The incident ion energy is given by the sum of the bias voltage and the initial ion energy of the carbon ions (20 eV [3]). The substrate holder could be heated and the temperature was monitored with a thermocouple. The substrates were held at the deposition temperature for at least 1 h prior to deposition. A series of films was deposited at base pressure, 2×10^{-4} mbar nitrogen partial pressure and 10^{-3} mbar nitrogen partial pressure varying the deposition temperature from room temperature to 300°C. All films deposited at temperatures above room temperature were deposited at floating potential.

The nitrogen content of films with over 2% nitrogen was determined by elastic recoil detection analysis (ERDA). Secondary ion mass spectroscopy (SIMS) was used for samples with lower nitrogen contents. The SIMS data were calibrated by comparing the ratio of the CN^- ion signal to that of carbon ions for samples of known nitrogen content measured previously by ERDA.

For EELS measurements, samples were deposited on Si substrates to a thickness of 30 nm, the Si etched away and free-standing ta-C films mounted on copper grids. The measurements were performed in transmission with a purpose-built spectrometer with a primary energy of 170 keV [8]. The sp^3 content is derived from the carbon K edge by comparing the ratio of areas of the 285 eV peak and the 290 eV edge [9].

Raman measurements were performed on a Renishaw Raman microscope system 2000 and on a Jobin-Yvon T64000 spectrometer, using the 514 nm wavelengths of an Ar ion laser or the 532 nm of a frequency doubled Nd:YAG laser. The spectra in general show two features, a G peak at $1540\text{--}1600\text{ cm}^{-1}$ and a D peak around 1350 cm^{-1} . The spectra were fitted with a Breit–Wigner–Fano (BWF) function $\{I(\omega) = I_0(\omega)[1 + 2(\omega - \omega_0)/q\Gamma]^2 / [1 + 2(\omega - \omega_0)/\Gamma]^2\}$ for the G peak and a Lorentzian function for the D peak. The G peak position is given by the maximum rather than the centre of the BWF function. The size of the D peak arises from graphitic clustering of sp^2 sites, and to quantify this the $I(\text{D})/I(\text{G})$ ratio was calculated as the intensities of the D and G peaks.

The optical band gap was determined from transmission and reflection spectra using an Ati-UNICAM UV–visible spectrometer. For conductivity measurements, Al electrode gap-cells were evaporated on the films on quartz substrates and a Hewlett Packard 4140B pA meter was used for I – V measurements. The conductivity was determined over the temperature range from room temperature to 200°C to derive the activation energy.

3. Results and discussion

3.1. Nitrogen content of samples

Fig. 1 shows the variation of nitrogen content of samples deposited at room temperature and at 100 eV ion energy as a function of the nitrogen partial pressure in the FCVA system. A fit to the linear region of our data reveals that the nitrogen/carbon atom ratio x_{N} (at%) varies as a slightly sublinear function of p_{N_2} (mbar):

$$x_{\text{N}} \approx 4500 \times (p_{\text{N}_2})^{0.9}.$$

Thus the films deposited at room temperature have a nitrogen content ranging from 0.01% to 8%. Fig. 1 also includes other data [10–13] for comparison. The films of Chhowalla and Hartmann were deposited using an unfiltered arc, while Stanishevsky and Shi used deposition systems similar to our work. As the nitrogen pressure rises above about 0.01 mbar, the nitrogen content saturates or even decreases for filtered and unfiltered arc systems. This limits the maximum N content of films produced by a single gun FCVA to about 35 at%.

It is believed that the plasma beam is highly ionised after the filter bend and that the deposition mechanism of carbon and nitrogen is mainly due to ions. In this case the N^+/N_2 or N_2^+/N_2 fraction is a constant in the observed pressure range up to 10^{-3} mbar. The saturation and decline of N incorporation at higher p_{N_2} might be explained by a reduction of ionisation due to recombination processes. It is unlikely that neutral N_2 can be incorporated into the growing films. It was also found that higher background pressures in arc systems shift the ion energies to lower values [14], and recently it was proposed by Morrison et al. [15] that high-energy nitrogen species (100 eV) can get implanted into the ta-C matrix, while low-energy nitrogen species tend to etch it. As at higher pressures there will be more low-energy species, etching of the carbon matrix by nitrogen might be another reason for the saturation and decline of nitrogen content with pressure.

3.2. Room temperature deposition: variation with nitrogen content

Fig. 2 shows the variation of sp^3 content (at the C site) deposited at room temperature and 100 eV as a function of nitrogen content. The sp^3 fraction is seen to remain at about 80% up to 9% N content. At higher nitrogen contents it starts to decrease sharply. Similar results have been found by Davis et al. [16]. For pulsed laser deposited (PLD) carbon. Hu et al. found a transition from sp^3 to sp^2 at 12% nitrogen concentration [17].

Fig. 3a shows the position of the G peak as a function of N content. A small contribution from the D peak is

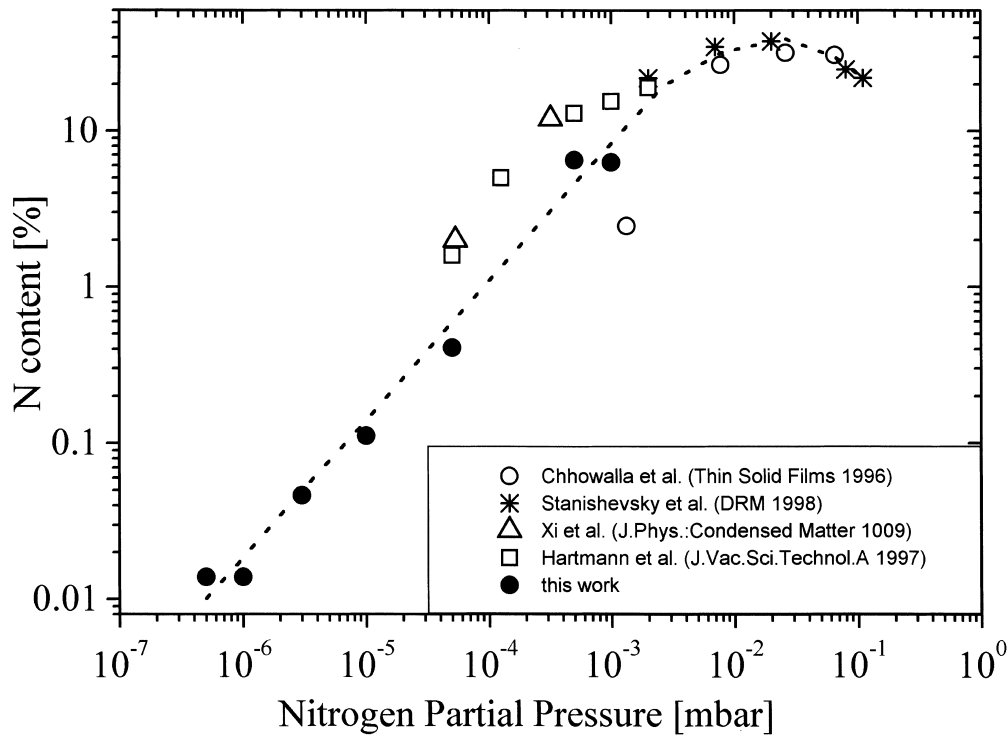


Fig. 1. Nitrogen content vs. nitrogen partial pressure of this work and others.

visible at pressures above 10^{-4} mbar, however, for consistency the spectra were fitted with BWF functions only. The G peak is seen to decrease from 1575 cm^{-1} as in pure ta-C to 1540 cm^{-1} for a nitrogen content of about 8%. We can interpret the data by assuming nitrogen helps to create larger sp^2 clusters. Fig. 3b shows the q factor for samples with more than 0.1% nitrogen (below this value the q factor is $>10^6$). The q factor is a measure for the symmetry of the peak: the smaller the value of q the more asymmetric the peak and the broader the sp^2 chain length distribution [18]; it can clearly be seen to continuously decrease with nitrogen content.

The increasing asymmetry can be interpreted as a slowly increasing broad D peak, an indication of the formation of ring structures.

In accordance with the above interpretation, the G peak width (G width) increases as the G shift decreases.

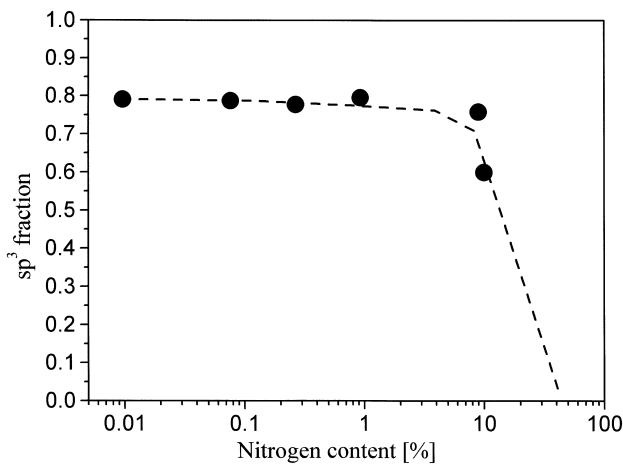


Fig. 2. sp^3 fraction vs. nitrogen content for room temperature deposition. The dotted line is a guide to the eye only.

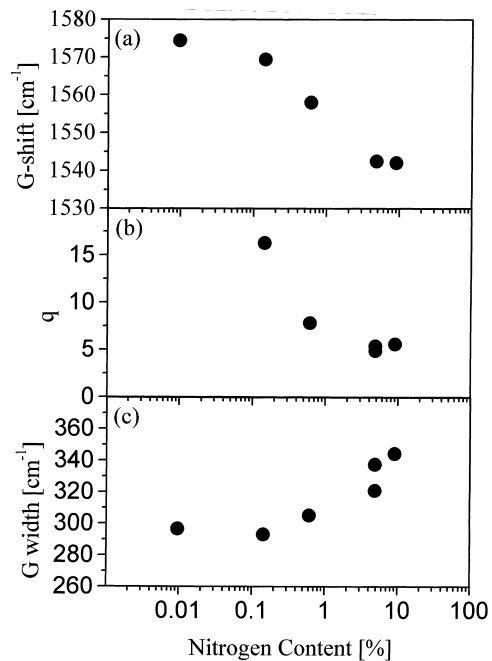


Fig. 3. (a) Raman G position vs. N content, (b) q factor of BWF fit vs. N content for room temperature deposition, and (c) G width vs. N content.

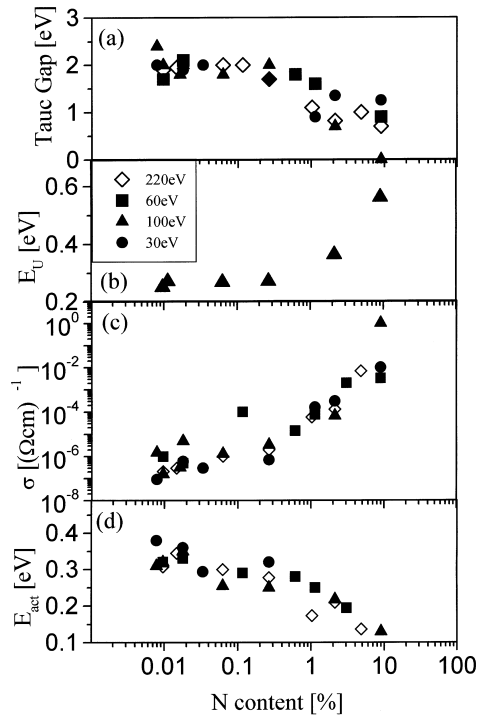


Fig. 4. (a) Optical gap, (b) Urbach energy, (c) room temperature conductivity and (d) conductivity activation energy vs. N content, for room temperature deposition.

The broadening of the G width indicates a broad distribution of oscillation modes. So even though the sp^2 content increases very slightly, the sp^2 sites do not ‘graphitise’ (order into graphite-like clusters), but the variation of sp^2 bonds becomes larger. The broadening of Raman peaks due to nitrogen was also observed by Hellgren et al. [5].

Fig. 4a shows the optical band gap determined by reflection–transmission methods, as a function of N content for samples deposited at various ion energies. The gap remains above about 2.0 eV up to a N content of 0.4%, and then decreases gradually with further N addition. In some cases an initial increase in the gap from 0.01% containing samples to 0.04% nitrogen containing samples could be observed.

Photothermal deflection spectroscopy (PDS) measurements were performed to determine the optical absorption edge. The absorption edge shows a roughly exponential region, whose energy width is called the Urbach energy E_U . The absorption coefficient varies steadily with photon energy, without the clear distinction between band and tail regions seen in amorphous silicon, so E_U is defined at 1 eV. Fig. 4b shows E_U as a function of N content, where a sudden increase occurs for N contents over 1%, indicating a broadening of the band edges. This increase in disorder is believed to be due to the broadening of sp^2 chain length distribution observed in the decrease of the G peak position and the increase of the G width, which correlate with E_U .

Fig. 4c and d shows the conductivity and conductivity activation energy (taken at 300 K) of these films. Samples deposited at room temperature with no nitrogen show a room temperature conductivity of $10^{-6} (\Omega \text{ cm})^{-1}$. The conductivity increases slowly with N content to $10^{-4} (\Omega \text{ cm})^{-1}$ at 1% N, and then increases more quickly to reach about $1 (\Omega \text{ cm})^{-1}$ at 9% N. Fig. 4d shows that most samples have a slight maximum in the activation energy at a p_{N_2} of 10^{-6} mbar. In two sets of samples, a slight increase in optical gap is also seen at this p_{N_2} . It is believed that as-deposited ta-C is p-type and that the Fermi level moves through midgap at a nitrogen concentration of 0.01%, coinciding with the maximum of activation energy. Heterostructures on silicon also suggested that nitrogen acts as a substitutional dopant of ta-C [19], and recently scanning tunneling microscopy showed a movement of the Fermi level through midgap [20] as well as thin film transistors made out of ta-C with changing N fraction [21].

3.3. Depositions at elevated temperature

It was found before that ta-C changes rapidly from sp^3 -rich to sp^2 -rich at a certain transition deposition temperature. The transition temperature was found to be dependent on incident ion energy [3,4], as well as on instantaneous deposition rate using a pulsed arc [22].

Fig. 5a shows the $I(D)/I(G)$ ratio for films deposited

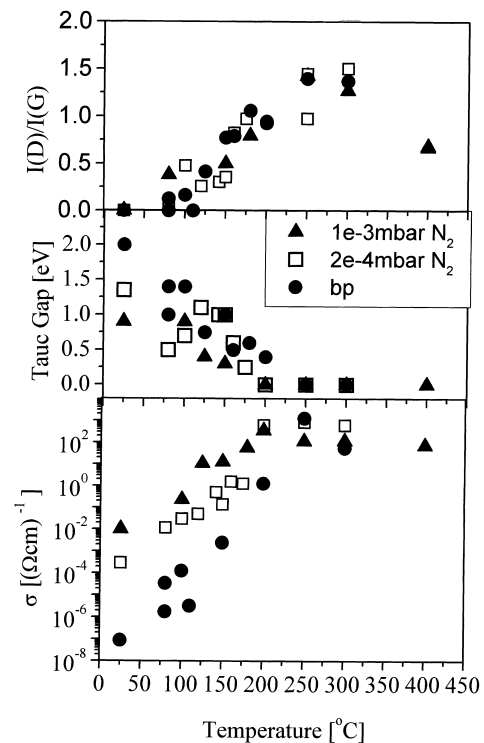


Fig. 5. (a) $I(D)/I(G)$, (b) optical band gap (Tauc), and (c) conductivity vs. deposition temperature for samples deposited at different nitrogen partial pressures.

at three different nitrogen pressures. The results show the appearance of a D peak at deposition temperatures above 80°C and a steady increase in the $I(D)/I(G)$ ratio up to temperatures of 250°C. Above this temperature the $I(D)/I(G)$ ratio seems to level off. One sample was deposited at a nitrogen partial pressure of 10^{-3} mbar at 400°C, which shows a decrease of $I(D)/I(G)$. No trend of change in transition temperature with nitrogen partial pressure could be made out, which means that the effects of enhancing the sp^2 fraction of films for elevated deposition temperature and nitrogen are independent of each other. It was also observed that the G width decreases from 300 cm^{-1} to 200 cm^{-1} for temperatures between room temperature and 200°C. For higher temperatures the G width remains constant. The decrease of G width also seems independent of nitrogen partial pressure. Nitrogen seems to induce a broader variation of sp^2 bond lengths and enhance clustering, while leaving the surrounding sp^3 matrix intact. Deposition at higher temperatures seems to increase the sp^2 content of the carbon matrix independently of nitrogen content. At elevated temperatures the decrease in G width means that the sp^2 clusters become more ordered.

Fig. 5b and c shows the optical band gap and conductivity vs. deposition temperature. The optical gap is seen to decrease steadily with increasing T_s ; samples with higher N content show a smaller gap. Between room temperature and 200°C the conductivity increases linearly and depends strongly on N partial pressure. Above 200°C the conductivity levels off at about $100\text{ (}\Omega\text{ cm)}^{-1}$, i.e. becomes almost independent of N partial pressure, and its dependence on temperature declines.

The optical gap is more sensitive to deposition temperature than the conductivity: samples deposited at room temperature clearly show a higher gap than samples deposited at 80°C. Samples above deposition temperatures of 200°C did not show an optical gap any more.

3.4. Phase diagram

The previous discussed results make it possible to extend the phase diagram for sputter deposited a-C:N films proposed by Hellgren et al. [5] to films deposited by cathodic arc systems. Doping in ta-C can only be found in sp^3 -rich samples, which is at deposition temperatures below 100°C and below a nitrogen concentration of 0.4% where sp^2 sites have not clustered. The doping regime is surrounded by a regime where the sp^3 matrix is still intact, but sp^2 sites have started to cluster. Temperatures above 200°C let the samples become graphitic, while high nitrogen pressures lead to a sp^2 matrix, but with a broad distribution of cluster sizes. Fullerene-like structures can be observed in vacuum arc deposition systems at high nitrogen pressures, but the influence of temperature on these structures is still not clear.

4. Conclusions

In a filtered cathodic vacuum arc the nitrogen incorporation into ta-C films is nearly linear with nitrogen partial pressure in the system up to pressures of 10^{-3} mbar. The maximum nitrogen content in a-C films achievable with this method is limited to 35%. The sp^3

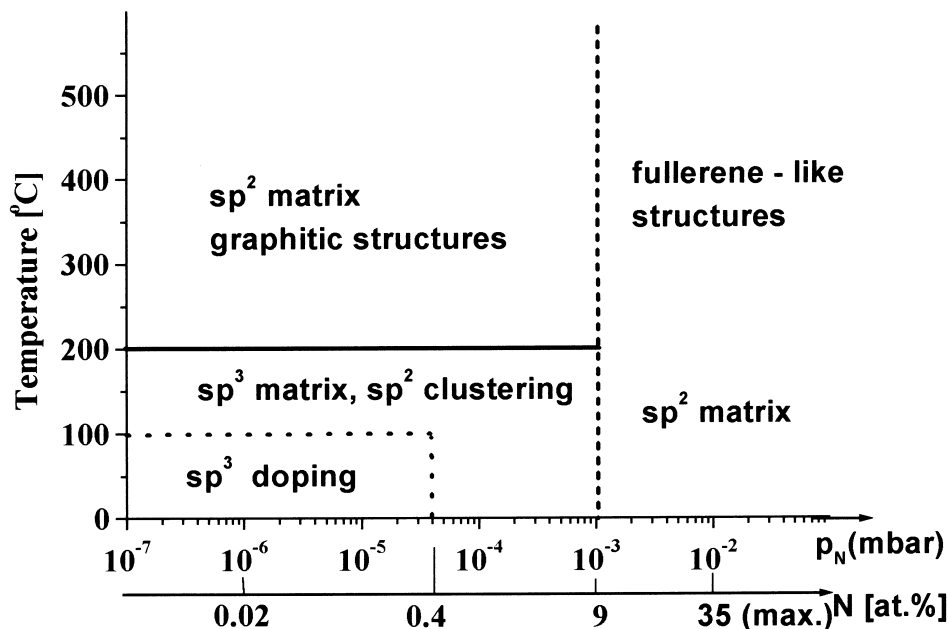


Fig. 6. Schematic phase diagram for FCVA depositions of a-C in nitrogen atmosphere.

content stays nearly constant for up to 9% nitrogen concentration. Up to 9% nitrogen in ta-C films, N enhances the formation of sp^2 clusters with a broad variety of bond lengths. The surrounding sp^3 matrix is almost unaffected by nitrogen up to this level. Nitrogen in FCVA deposited amorphous carbon does not change its transition temperature, indicating that temperature is a more important parameter for the initiation of the formation of sp^2 sites than nitrogen. A phase diagram for FCVA deposited a-C in a nitrogen atmosphere has been proposed (Fig. 6).

Acknowledgements

The authors want to acknowledge the help of M. Siegal, Sandia National Laboratories, H. Busch, University of Bonn, M. Mooney, NMRC, Cork, M. Stutzmann and C. Nebel, WSI, Munich, C.E. Bottani of Politecnico di Milano and D. Richards of Cavendish Laboratories, Cambridge. The authors also acknowledge LSF funding from the European Union. B.K. and A.C.F. acknowledge funding by the European Union's TMR Marie Curie Fellowships.

References

- [1] J. Robertson, C.A. Davis, *Diamond Relat. Mater.* 4 (1995) 441.
 [2] Y. Lifshitz, *Diamond Relat. Mater.* 5 (1996) 388.
 [3] M. Chhowalla, J. Robertson, C.W. Chen, S.R.P. Silva, C.A.

- Davis, G.A.J. Amaratunga, W.I. Milne, *J. Appl. Phys.* 81 (1997) 139.
 [4] S. Sattel, J. Robertson, H. Ehrhardt, *J. Appl. Phys.* 82 (1997) 1.
 [5] N. Hellgren, M.P. Johansson, E. Broitman, L. Hultman, J.-E. Sundgren, *Phys. Rev. B* 59 (1999) 5162.
 [6] G.A.J. Amaratunga, M. Chhowalla, C.J. Kiely, I. Alexandrou, R. Aharonov, R.M. Devenish, *Nature* 383 (1996) 321.
 [7] P.J. Fallon, V.S. Veerasamy, C.A. Davis, J. Robertson, G.A.J. Amaratunga, W.I. Milne, J. Koskinen, *Phys. Rev. B* 48 (1993) 4777.
 [8] J. Fink, *Adv. Electron. Electron Phys.* 75 (1989) 121.
 [9] S.D. Berger, D.R. McKenzie, P.J. Martin, *Philos. Mag. Lett.* 57 (1988) 285.
 [10] M. Chhowalla, I. Alexandrou, C. Kiely, G.A.J. Amaratunga, R. Aharonov, R.F. Fontana, *Thin Solid Films* 290/291 (1996) 103.
 [11] A. Stanishevsky, L. Khriatchchev, I. Akula, *Diamond Relat. Mater.* 7 (1998) 1190.
 [12] X. Shi, H. Fu, J.R. Shi, L.K. Cheah, B.K. Tay, P. Hui, *J. Phys.: Condens. Matter* 10 (1998) 9293.
 [13] J. Hartmann, P. Siemroth, B. Schultrich, B. Rauschenbach, *J. Vac. Sci. Technol. A* 15 (1997) 2983.
 [14] M.M.M. Bilek, P.J. Martin, D.R. McKenzie, *J. Appl. Phys.* 83 (1998) 2965.
 [15] N.A. Morrison, S.E. Rodil, J. Robertson, W.I. Milne, to be published in *Philos. Mag. B*.
 [16] C.A. Davis, D.R. McKenzie, Y. Yin, E. Kravtchinskaja, G.A.J. Amaratunga, V.S. Veerasamy, *Philos. Mag. B* 69 (1994) 1133.
 [17] J. Hu, P. Yang, C.M. Lieber, *Phys. Rev. B* 57 (1998) R3185.
 [18] S. Praver, K.W. Nugent, Y. Lifshitz, G.D. Lempert, E. Grossman, J. Kulik, I. Avigal, R. Kalish, *Diamond Relat. Mater.* 5 (1996) 433.
 [19] G.A.J. Amaratunga, D.E. Segal, D.R. McKenzie, *Appl. Phys. Lett.* 59 (1991) 69.
 [20] C. Arena, B. Kleinsorge, J. Robertson, W.I. Milne, M.E. Welland, *J. Appl. Phys.* 85 (1999) 1609.
 [21] S.L. Maeng et al., *Diamond Relat. Mater.* (1999) in press.
 [22] J. Koskinen, J.-P. Hirvonen, J. Keränen, *J. Appl. Phys.* 84 (1998) 648.